Research Article

Quality and Reliability Engineering International

(wileyonlinelibrary.com) DOI: 10.1002/qre.1536

Published online in Wiley Online Library

Monitoring General Linear Profiles When Random Errors Have Contaminated Normal Distributions

Longcheen Huwang,[a*†] Yi-Hua Tina Wang[b] and Cheng-Che Shen[a]

We consider the quality of a process which can be characterized by a general linear profile where the random error has a contaminated normal distribution. On the basis of trimmed least squares estimation, new control charts for monitoring the coefficient parameters and/or the error variance of the profile are proposed. Simulation studies show that the proposed control charts outperform the existing competitors under such a profile. An example from manufacturing facility is used to illustrate the applicability of the proposed charts. Copyright © 2013 John Wiley & Sons, Ltd.

Keywords: trimmed least squares estimation; average run length; control chart; EWMA; out-of-control; Phase I; Phase II

1. Introduction

Statistical process control (SPC) has been successfully applied to monitor various industrial processes. In most SPC applications, the quality of a process can be adequately represented by the distribution of a univariate quality characteristic or by the multivariate distribution of a vector consisting of a few quality characteristics. In many applications, however, the quality of a process or product is characterized and summarized better by a relationship (or profile) between the response variable and one or more explanatory variables; that is, the main topic is on monitoring the profile that represents such a relationship, instead of on monitoring a single quality characteristic or several quality characteristics.

For monitoring the simple linear profiles, Kang and Albin[1] proposed two different control charting schemes in Phase I and Phase II monitoring. One of them is a multivariate T^2 chart, and the other is the combination of an exponentially weighted moving average (EWMA) chart and a range (R) chart. Kim *et al.*[2] proposed using a combination of three EWMA charts to, respectively, detect a shift in the intercept, slop, and standard deviation simultaneously in Phase II monitoring. They also proposed applying similar Shewhart-type control charts in Phase I monitoring. Gupta *et al.*[3] compared the performance of the control charts proposed by Croarkin and Varner[4] and Kim *et al.*[2] for monitoring simple linear profiles in Phase II study. They concluded that the combined EWMA charts of Kim *et al.*[2] are better than the charting scheme of Croarkin and Varner[4]. Mahmoud and Woodall[5] studied several control charting schemes for monitoring simple linear profiles in Phase I study. Zou *et al.*[6] proposed a control charting scheme on the basis of a change point model for monitoring simple linear profiles where the process parameters are unknown but can be estimated from the in-control (IC) historical data. Mahmoud *et al.*[7], based on likelihood ratio statistics, proposed a change point method for detecting sustained shifts in simple linear profiles in Phase I study. Zou *et al.*[8] studied a self-starting control chart for monitoring simple linear profiles when the process parameters are unknown but some IC data in Phase I study are available. For monitoring general linear profiles, Zou *et al.*[9] applied an MEWMA single chart to the transformations of estimated profile parameters in Phase II study. More studies for monitoring linear profiles can be found in the literature. See, e.g. Jensen *et al.*[10]; Mestek *et al.*[11]; Stover and Brill[12]; Lawless *et al.*[13]; Wang and Huwang[14].

Although monitoring the linear profiles is an important issue, in many practical applications, the profiles cannot be represented by linear models adequately. Walker and Wright[15] studied vertical density profiles which apparently cannot be represented by linear profiles. Woodall *et al.*[16] proposed control charts to monitor the same vertical density profiles. Williams *et al.*[17] developed three general approaches to the formulation of T^2 statistics based on nonlinear model estimation in Phase I study. Colosimo and Pacella[18] employed principal component analysis to identify systematic patterns in roundness profiles. Williams *et al.*[19] utilized data from DuPont to monitor dose–response profiles used in high-throughput screening based on the nonlinear model approaches of Williams *et al.*[17], where a four-parameter logistic regression model was used to describe the profiles. Yeh *et al.*[20] proposed Phase I profile monitoring schemes for binary responses that could be represented by the logistic regression model. Shang *et al.*[21]developed a

[a]Institute of Statistics, National Tsing Hua University, Hsinchu, Taiwan
[b]Department of Statistics, Tamkang University, Tamsui, Taiwan
*Correspondence to: Longcheen Huwang, National Tsing Hua University, Hsinchu, Taiwan
†E-mail: huwang@stat.nthu.edu.tw

control chart by integrating the EWMA scheme and the likelihood ratio test based on the logistic regression model in Phase II study. Jin and Shi[22] applied dimension-reduction techniques to study a stamping tonnage profile, which apparently is a nonlinear profile. Lada *et al.*[23] and Ding *et al.*[24] used dimension-reduction techniques, including wavelet and independent component analysis to study a general category of nonlinear profiles.

Recently, Zou *et al.*[25] integrated a MEWMA procedure with a generalized likelihood ratio test (Fan *et al.*[26]) based on the local linear smoother of Fan and Gijbels[27] to develop a nonparametric control chart for monitoring general smooth regression profiles. Qiu *et al.*[28] proposed monitoring smooth profiles which can be described by a nonparametric mixed-effects model to account for the within-profile correlation. Zi *et al.*[29] developed a distribution-free and robust method for monitoring linear profiles.

In this article, we focus on a study of Phase II monitoring for general linear profiles when random errors have contaminated normal distributions. To be specific, assume that for the jth sample collected overtime, we have the observations (X_j, $\boldsymbol{y_j}$), where $\boldsymbol{y_j} = (y_{1j}, y_{2j}, \ldots, y_{n_j j})'$ is an n_j-variate vector and X_j is a $n_j \times p$ ($n_j > p$) matrix. Precisely, when the process is in control, the underlying model is assumed to be

$$\boldsymbol{y_j} = X_j \boldsymbol{\beta} + \boldsymbol{\varepsilon}_j, \tag{1}$$

where $\boldsymbol{\beta} = (\beta_1, \beta_2, \ldots, \beta_p)'$ is a p-dimensional coefficient vector and $\boldsymbol{\varepsilon_j} = (\varepsilon_{1j}, \varepsilon_{2j}, \ldots, \varepsilon_{n_j j})'$ is a vector of independent, identically distributed random variables with mean 0, variance σ^2, and distribution function F. It is assumed that X_j is of form $(\mathbf{1}, X_j^*)$, where each column of X_j^* is orthogonal to $\mathbf{1}$ and $\mathbf{1}$ is an n_j-variate vector of all 1's. Otherwise, we can obtain this form through some appropriate transformations. The explanatory variable matrix X_j is usually the same for different j and the n_j's are equal in practical applications (hereafter X and n are used to replace X_j and n_j). Here, we assume that each random error ε_{ij}, $1 \le i \le n$, has a contaminated normal distribution (a mixture of normal distributions). In spite of the advantages, including efficiency when F is a normal distribution, of the least squares estimator of $\boldsymbol{\beta}$, this estimator is inefficient when F has a contaminated normal distribution, and the estimator possesses high sensitivity to spurious data. The presence of spurious observations can be modeled by letting F be a mixture of two normal distributions, i.e. $F \sim (1-k)N(\theta,\sigma^2) + kN(\varphi,\tau^2)$. When k is small, $\theta = \varphi, \tau^2 = c\sigma^2$ and c large, F is commonly used as a heavy-tailed alternative to a normal distribution. For example, the family of t distributions is of this type. (Write $t = GH$, where H is normal and G is independently distributed as the inverse of the square root of a chi-square divided by its degrees of freedom) On the other hand, if k is small, φ quite different from θ and τ small, then F generates outliers near the value φ. It is a common statistical practice to study the robustness of a statistical procedure by constructing a simple class of alternative mixture distributions. In the article, we will especially emphasize on the above two situations when F has a contaminated normal distribution. As illustrated by a real example from manufacturing facility in Section 5, general linear profiles can have random errors with contaminated normal distributions in realistic situations.

For the location model, three classes, M, L, and R of estimators have been suggested as alternatives to the traditional sample mean (see Lehmann[30] for an introduction). Among the L estimators, the trimmed mean is particularly attractive since it is efficient and easy to compute under most circumstances. Stigler[31] (p. 1070) applied robust estimators to data from 18th- and 19th-century experiments design to measure basic physical constants. He concluded that the 10% trimmed mean (the smallest nonzero trimming percentage used in the study) is preferable as the recommended estimator. Koenker and Bassett[32], who extended the concept of quantiles to the linear model, proposed a method of defining a regression analog to the trimmed mean. Let $0 < \alpha < 1$. For a certain random sample ($X, \boldsymbol{y}$) satisfying (1), where $\boldsymbol{y} = (y_1, y_2, \ldots, y_n)'$ and $X' = (\boldsymbol{x_1}, \boldsymbol{x_2}, \ldots, \boldsymbol{x_n})$, they defined the αth regression quantile, denoted by $\hat{\boldsymbol{\beta}}(\alpha)$, to be any solution to the minimization problem:

$$\min_{\boldsymbol{\beta} \in R^p} \{ \sum_{i \in A} (1-\alpha) |y_i - \boldsymbol{x}'_i \boldsymbol{\beta}| + \sum_{i \in A^c} \alpha |y_i - \boldsymbol{x}'_i \boldsymbol{\beta}| \}, A = \{ i : y_i - \boldsymbol{x}'_i \boldsymbol{\beta} < 0 \}. \tag{2}$$

They showed that the regression quantiles have asymptotic behavior similar to those of sample quantiles in the one-sample problem. For more literature reviews about regression quantiles, interested readers can see Koenker[33] and Koenker and Hallock[34]. As Koenker and Bassett[32] pointed out, regression quantiles can be computed by standard linear programming techniques (Meketon[35]). They also recommended the following trimmed least squares estimators ($\hat{\boldsymbol{\beta}}_{KB}(\alpha)$): Remove from the sample any data whose residual from $\hat{\boldsymbol{\beta}}(\alpha)$ is negative or whose residual from $\hat{\boldsymbol{\beta}}(1-\alpha)$ is positive and calculate the least squares estimator using the remaining data. Ruppert and Carroll[36] proposed another regression analog to the trimmed mean. The estimator is denoted by $\hat{\boldsymbol{\beta}}_{PE}(\alpha)$ for $0 < \alpha < 1$, which requires a preliminary estimator β_0. Define the residuals from the preliminary estimator $\hat{\boldsymbol{\beta}}_0$ as $r_i = y_i - \boldsymbol{x}'_i \hat{\boldsymbol{\beta}}_0$, $i = 1, 2, \ldots, n$. Let r_{1n} and r_{2n} be the $[n\alpha]$th and $[n(1-\alpha)]$th ordered residuals, respectively. Then, the estimator $\hat{\boldsymbol{\beta}}_{PE}(\alpha)$ is the least squares estimator that is calculated after all observations are removed that satisfy

$$r_i \le r_{1n} \text{ or } r_i \ge r_{2n}. \tag{3}$$

Suppose that the residuals from $\hat{\boldsymbol{\beta}}_0$ are calculated and that those data corresponding to the $[\alpha]$ smallest and $[\alpha]$ largest residuals are removed. Then, $\hat{\boldsymbol{\beta}}_{PE}(\alpha)$ is defined as the least squares estimator calculated from the remaining data. Ruppert and Carroll [36] showed that the distribution of the estimator $\hat{\boldsymbol{\beta}}_{PE}(\alpha)$ depends heavily on that of the preliminary estimator $\hat{\boldsymbol{\beta}}_0$. Surprisingly, if the preliminary estimate is either the least squares or least-absolute-deviation estimator, then $\hat{\boldsymbol{\beta}}_{PE}(\alpha)$ is inefficient at normal model. However, if the preliminary estimator $\hat{\boldsymbol{\beta}}_0$ is the average of the αth and $(1-\alpha)$th regression quantiles, they claimed that the estimators $\hat{\boldsymbol{\beta}}_{PE}(RQ(\alpha))$ (i.e. the estimator $\hat{\boldsymbol{\beta}}_{PE}(\alpha)$ with $\hat{\boldsymbol{\beta}}_0=(\hat{\boldsymbol{\beta}}(\alpha)+\hat{\boldsymbol{\beta}}(1-\alpha))/2$) and $\hat{\boldsymbol{\beta}}_{KB}(\alpha)$ have the same asymptotic distribution under the following assumptions: (i) F has a continuous density f that is positive on the support of F. (ii) The ith row of X, $\boldsymbol{x}'_i=(x_{i1},x_{i2},\ldots,x_{ip})$, satisfies $x_{i1}=1$ for $i=1,2,\ldots,n$ and $\sum_{i=1}^{n} x_{ij}=0$ for $j=2,\ldots,p$. (iii) $lim_{n\to\infty}\left(max_{l\le p,i\le n}(n^{-\frac{1}{2}}|x_{il}|)\right)=0$. (iv) There exists positive definite Q such that $lim_{n\to\infty}n^{-1}(X'X)=Q$. 5. $\left(\hat{\boldsymbol{\beta}}_0-\boldsymbol{\beta}-\theta\boldsymbol{e}\right)=O_p(n^{-\frac{1}{2}})$ for some constant θ, where $\boldsymbol{e}'=(1,0,\ldots,0)$ is a p-dimensional column vector. Precisely, they showed that if F is symmetric (i.e. f is symmetric about zero),

$$n^{\frac{1}{2}}\left(\hat{\boldsymbol{\beta}}_{\mathrm{PE}}(RQ(\alpha))-\boldsymbol{\beta}\right)\xrightarrow{L}N\left(\mathbf{0},Q^{-1}\sigma^2(\alpha,F)\right), \tag{4}$$

where

$$\sigma^2(\alpha,F)=(1-2\alpha)^{-2}\left(\int_{\xi_1}^{\xi_2}z^2dF+\alpha\left(\xi_1^2+\xi_2^2\right)\right),$$

$\xi_1=F^{-1}(\alpha)$, and $\xi_2=F^{-1}(1-\alpha)$. The above result also holds when $\hat{\boldsymbol{\beta}}_{PE}(RQ(\alpha))$ is replaced by $\hat{\boldsymbol{\beta}}_{KB}(\alpha)$. Let S be the sum of squares for residuals calculated from the trimmed sample, that is,

$$S=\boldsymbol{y}'\ B\left(I_p-X\left(X'\ BX\right)^{-}X'\right)B\boldsymbol{y}, \tag{5}$$

where B is a $n\times n$ diagonal matrix with $B_{ii}=0$ or 1 according to i satisfies (3) or not. Let $c_1=\boldsymbol{e}'(\hat{\boldsymbol{\beta}}(\alpha)-\hat{\boldsymbol{\beta}}_{PE}(RQ(\alpha)))$, $c_2=\boldsymbol{e}'(\hat{\boldsymbol{\beta}}(1-\alpha)-\hat{\boldsymbol{\beta}}_{PE}(RQ(\alpha)))$, and

$$s^2(\alpha,F)=(1-2\alpha)^{-2}\left((n-p)^{-1}S+\alpha\left(c_1^2+c_2^2\right)-\alpha^2(c_1+c_2)^2\right). \tag{6}$$

Rupport and Carroll[36] also showed that

$$s^2(\alpha,F)\xrightarrow{p}\sigma^2(\alpha,F). \tag{7}$$

2. Control charts for monitoring coefficient parameters

Zou *et al.*[9] proposed a MEWMA scheme to monitor a general linear profile where the $p+1$ parameters, the p coefficients and the standard deviation σ, are controlled jointly in Phase II study. Based on model (1), for the jth sample $(X,\boldsymbol{y}_j)$ they defined

$$\boldsymbol{Z}_j(\beta)=\left(\hat{\boldsymbol{\beta}}_{LS,j}-\boldsymbol{\beta}\right)/\sigma \tag{8}$$

and

$$Z_j(\sigma)=\Phi^{-1}\left\{G\left((n-p)\hat{\sigma}^2_{LS,j}/\sigma^2;n-p\right)\right\}, \tag{9}$$

where $\hat{\boldsymbol{\beta}}_{LS,j}=\left(X'X\right)^{-1}X'\boldsymbol{y}_j, \hat{\sigma}^2_{LS,j}=(n-p)^{-1}(\boldsymbol{y}_j-X\hat{\boldsymbol{\beta}}_{LS,j})'\left(\boldsymbol{y}_j-X\hat{\boldsymbol{\beta}}_{LS,j}\right), \Phi^{-1}(\cdot)$ is the inverse of the standard normal distribution function, and $G(\cdot;\nu)$ is the chi-squared distribution function with ν degrees of freedom. Denote the $p+1$-variate random vector $\boldsymbol{Z}_j$ by $(\boldsymbol{Z}_j(\boldsymbol{\beta}),Z_j(\sigma))'$. Then, the vector is a multivariate random vector with mean $\mathbf{0}$ and covariance matrix $\Sigma=\begin{pmatrix}(X'\ X)^{-1} & \mathbf{0}\\ \mathbf{0} & 1\end{pmatrix}$ when the process is in control and F is normal. They used the charting statistic

$$\boldsymbol{W}_j=\lambda\boldsymbol{Z}_j+(1-\lambda)\boldsymbol{W}_{j-1}, j=1,2,\ldots, \tag{10}$$

where $\boldsymbol{W}_0$ is a starting vector and λ is a smoothing constant. The MEWMA chart triggers a signal if

$$U_j=\boldsymbol{W}'_j\ \Sigma^{-1}\boldsymbol{W}_j>L\frac{\lambda}{2-\lambda}, \tag{11}$$

where $L>0$ is determined to achieve the desired IC ARL. The charting scheme of Zou *et al.*[9] can be treated as a special case of MEWMA charts. The MEWMA chart was first invented by Lowry *et al.*[37]. Prabhu and Runger[38] studied the design of MEWMA charts.

Note that unlike the approach of Zou *et al.*[9] for which a single MEWMA chart is used to monitor the vector of coefficient parameters $\boldsymbol{\beta}$ and the standard deviation σ simultaneously, in the article, we will propose two separate control charts for monitoring $\boldsymbol{\beta}$ and σ, respectively, because there is no appropriate transformation like (9) under the assumption that F has a contaminated normal

Table I. Simulated values of $E(lns^2(\alpha,F))$

(k,b)	$\alpha=0$	$\alpha=0.05$	$\alpha=0.1$	$\alpha=0.15$	$\alpha=0.25$
(0,1)	−0.056	0.044	0.052	0.067	0.104
(0.05,3)	0.207	0.261	0.204	0.182	0.196
(0.05,5)	0.480	0.472	0.303	0.230	0.221
(0.05,10)	1.021	0.915	0.473	0.292	0.242
(0.1,3)	0.432	0.460	0.358	0.304	0.290
(0.1,5)	0.895	0.841	0.572	0.422	0.347
(0.1,10)	1.750	1.583	0.955	0.607	0.404
(0.25,3)	0.948	0.962	0.810	0.701	0.607
(0.25,5)	1.714	1.667	1.349	1.089	0.815
(0.25,10)	2.937	2.833	2.277	1.771	1.109

distribution. Here, we use the concept of the charting scheme of Zou *et al.*[9] but with a different estimator for monitoring the vector of coefficient parameters $\boldsymbol{\beta}$. Define

$$\boldsymbol{Z}_{PE,j}(\boldsymbol{\beta}) = \left(\hat{\boldsymbol{\beta}}_{PE,j}(RQ(\alpha)) - \boldsymbol{\beta}\right)/\sigma(\alpha,F) \tag{12}$$

and

$$\boldsymbol{W}_{PE,j} = \lambda \boldsymbol{Z}_{PE,j}(\boldsymbol{\beta}) + (1-\lambda)\boldsymbol{W}_{PE,j-1}, j = 1,2,\ldots, \tag{13}$$

where $\hat{\boldsymbol{\beta}}_{PE,j}(RQ(\alpha))$ is the trimmed least squares estimator of $\boldsymbol{\beta}$ proposed by Rupport and Carroll[36] based on the jth sample, $\boldsymbol{W}_{PE,0}$ is a p-dimensional starting vector, and λ is the smoothing constant. The chart signals if

$$U_{PE,j} = \boldsymbol{W}'_{PE,j}\left(X'X\right)\boldsymbol{W}_{PE,j} > L_{\boldsymbol{\beta}}\frac{\lambda}{2-\lambda}. \tag{14}$$

In the paper, the smoothing constant λ is chosen to be .2 which is consistent with Kim *et al.* [2], Zou *et al.* [9], and most of the EWMA schemes in the literature. Generally, a smaller value of λ causes more timely detection of smaller profile shifts. The initial vector $\boldsymbol{W}_{PE,0}$ is taken to be the zero vector, and the control limit $L_{\boldsymbol{\beta}}$ is decided by the IC ARL and the smoothing constant λ.

3. Control charts for monitoring coefficient parameters and standard deviation simultaneously

In the article, we assume that the distribution function F of the random errors has a contaminated normal distribution. Apparently, it is not appropriate to use the charting statistic of the variance transformation (9) to monitor the standard deviation σ of F. Since the standard deviation σ is positive, it is a common practice to use the log transformation to obtain a better normal approximation. Define

$$Z_{PE,j}(\sigma) = \frac{\log s_j^2(\alpha,F) - E\left(\log s_j^2(\alpha,F)\right)}{\sqrt{Var\left(\log s_j^2(\alpha,F)\right)}}, \tag{15}$$

Table II. Simulated values of $Var(lns^2(\alpha,F))$

(k,b)	$\alpha=0$	$\alpha=0.05$	$\alpha=0.1$	$\alpha=0.15$	$\alpha=0.25$
(0,1)	0.118	0.125	0.149	0.177	0.280
(0.05,3)	0.239	0.202	0.188	0.195	0.287
(0.05,5)	0.536	0.398	0.273	0.225	0.293
(0.05,10)	1.434	1.065	0.555	0.316	0.304
(0.1,3)	0.298	0.254	0.227	0.220	0.298
(0.1,5)	0.650	0.531	0.398	0.305	0.319
(0.1,10)	1.497	1.279	0.950	0.597	0.368
(0.25,3)	0.312	0.302	0.297	0.291	0.341
(0.25,5)	0.519	0.525	0.559	0.521	0.456
(0.25,10)	0.782	0.854	1.141	1.194	0.830

Table III. Upper control limits $H = L\lambda/(2-\lambda)$ and $H_\beta = L_\beta\lambda/(2-\lambda)$of the MEWMA and proposed charts respectively for monitoring coefficient parameters when $n = 20, \lambda = 0.2$ and IC ARL≈100

(k,b)	H	$H_\beta(\alpha = 0.05)$	$H_\beta(\alpha = 0.1)$	$H_\beta(\alpha = 0.15)$	$H_\beta(\alpha = 0.25)$
(0,1)	0.897	0.946	0.981	0.989	0.991
	(99.589)	(100.2967)	(100.123)	(99.891)	(99.930)
(0.05,3)	0.924	0.979	1.013	1.008	1.005
	(99.852)	(100.007)	(100.168)	(100.083)	(100.015)
(0.05,5)	0.992	1.100	1.057	1.031	1.018
	(99.347)	(99.92665)	(99.866)	(100.196)	(99.886)
(0.05,10)	1.120	1.880	1.173	1.069	1.035
	(100.283)	(99.824)	(99.712)	(100.613)	(100.234)
(0.1,5)	0.978	1.378	1.193	1.108	1.070
	(100.540)	(100.243)	(99.992)	(99.992)	(99.745)
(0.1,10)	1.030	3.177	1.853	1.279	1.122
	(100.272)	(100.118)	(100.013)	(99.279)	(99.694)
(0.25,5)	0.939	1.203	1.608	1.486	1.302
	(99.836)	(99.910)	(99.859)	(99.973)	(100.316)
(0.25,10)	0.950	1.259	3.123	3.198	1.876
	(100.386)	(100.237)	(99.927)	(100.237)	(100.373)

Parentheses contain the corresponding IC ARLs.

Table IV. Upper control limits $H = L\lambda/(2-\lambda)$ of the MEWMA chart and $H_\beta = L_\beta\lambda/(2-\lambda)$ and $H_\sigma = L_\sigma\lambda/(2-\lambda)$ of the proposed chart for monitoring coefficient parameters and standard deviation, simultaneously when $n = 20, \lambda = 0.2$ and IC ARL ≈100

		$\alpha = 0.05$	$\alpha = 0.1$	$\alpha = 0.15$	$\alpha = 0.25$
(k,b)	H	H_β H_σ	H_β H_σ	H_β H_σ	H_β H_σ
(0,1)	1.136	1.048	1.087	1.098	1.099
	(99.988)	0.935	0.933	0.939	0.941
		(99.970)	(100.078)	(99.979)	(99.625)
(0.05,3)	1.195	1.084	1.122	1.116	1.118
	(99.950)	0.952	0.948	0.943	0.947
		(100.159)	(100.331)	(99.797)	(100.053)
(0.05,5)	1.290	1.226	1.178	1.145	1.132
	(100.175)	0.949	0.974	0.962	0.948
		(100.153)	(100.691)	(100.179)	(99.859)
(0.05,10)	1.410	2.180	1.318	1.185	1.153
	(99.918)	0.908	1.007	1.052	0.955
		(100.396)	(100.159)	(100.210)	(100.472)
(0.1,5)	1.220	1.548	1.333	1.234	1.195
	(100.021)	0.913	0.941	0.958	0.952
		(100.308)	(100.163)	(100.243)	(100.109)
(0.1,10)	1.249	3.655	2.145	1.452	1.252
	(99.923)	0.884	0.918	1.000	0.985
		(100.672)	(99.710)	(100.763)	(99.859)
(0.25,5)	1.157	1.352	1.819	1.687	1.466
	(100.243)	0.912	0.905	0.915	0.944
		(100.189)	(100.276)	(100.589)	(100.090)
(0.25,10)	1.181	1.430	3.620	3.755	2.206
	(100.214)	0.939	0.898	0.886	0.952
		(100.238)	(100.543)	(100.672)	(100.298)

Parentheses contain the corresponding IC ARLs.

where $s_j^2(\alpha, F)$ is computed based on (6) using the jth profile data. Due to the difficulty of deriving the exact distribution of $s_j^2(\alpha, F)$, here we use statistical simulation to compute $E\left(\log s_j^2(\alpha, F)\right)$ and $Var\left(\log s_j^2(\alpha, F)\right)$. Tables I and II tabulate the simulated values of

$E\left(logs_j^2(\alpha,F)\right)$ and $Var\left(logs_j^2(\alpha,F)\right)$, respectively, for $n = 20$, $\alpha = 0, 0.05, 0.1, 0.15, 0.25$ and several contaminated normal distributions of F. The contaminated normal distributions of F have the form

$$F \sim (1-k)N(0,1) + kN\left(0,b^2\right), \tag{16}$$

where $0 \le k \le 1$ and $b \ge 1$. Note that this contaminated normal distribution is commonly used as a heavy-tailed alternative to the normal distribution. The results are based on 50,000 simulations. From the tables, we can see that for fixed k and α both $E(log\sigma^2(\alpha,F))$ and $Var\left(logs_j^2(\alpha,F)\right)$ are increasing in b. Consequently, we define

$$V_{PE,j} = \lambda Z_{PE,j}(\sigma) + (1-\lambda)V_{PE,j-1}, j = 1,2,\ldots, \tag{17}$$

where $V_{PE,0} = 0$. The variance chart signals if

$$\left|V_{PE,j}\right| > L_\sigma \frac{\lambda}{2-\lambda}, \tag{18}$$

where L_σ is determined to achieve a specified IC ARL. In order to monitor the whole profile, the two EWMA charts (14) and (18) are used jointly, and the profile change is detected as one of the two charts signals.

4. Performance comparisons

In this section, we compare the performance of the proposed and MEWMA charts for monitoring the coefficient parameters only and the coefficient parameters and standard deviation simultaneously. As for monitoring the coefficient parameters and

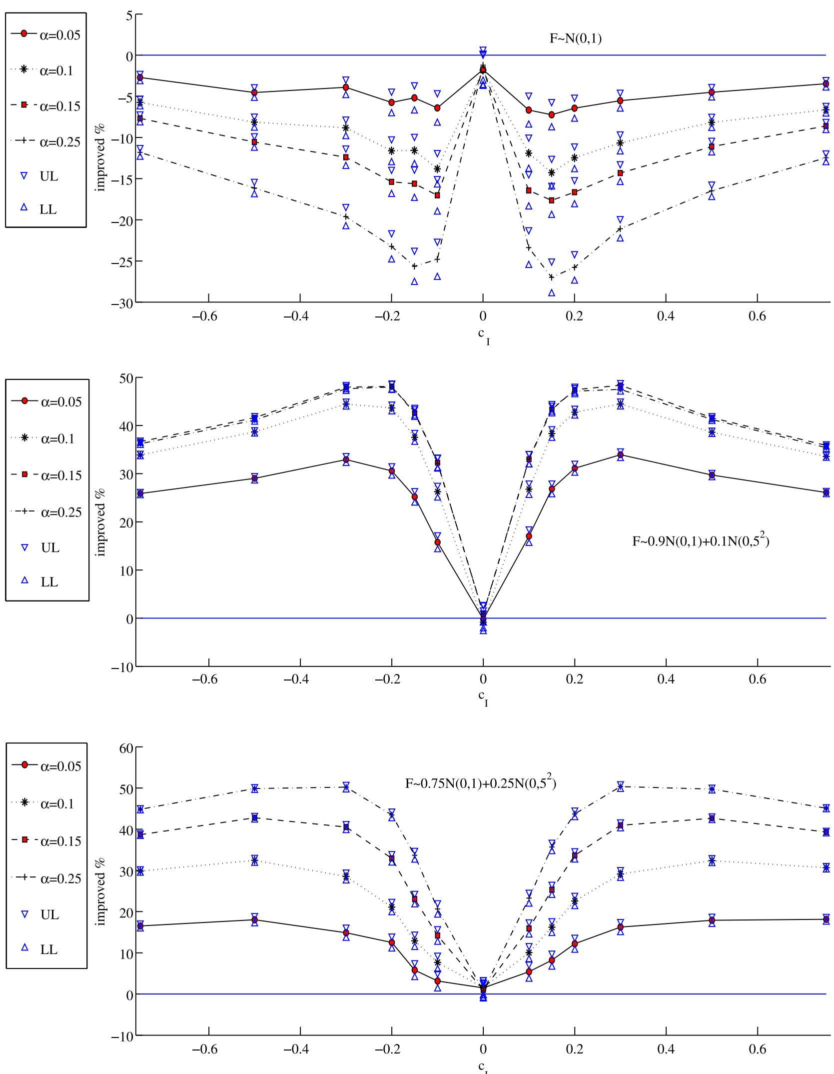

Figure 1. Improved percentages of the OC ARLs of the proposed charts for monitoring coefficient parameters when $\beta_0 \rightarrow \beta_0 + c_I$

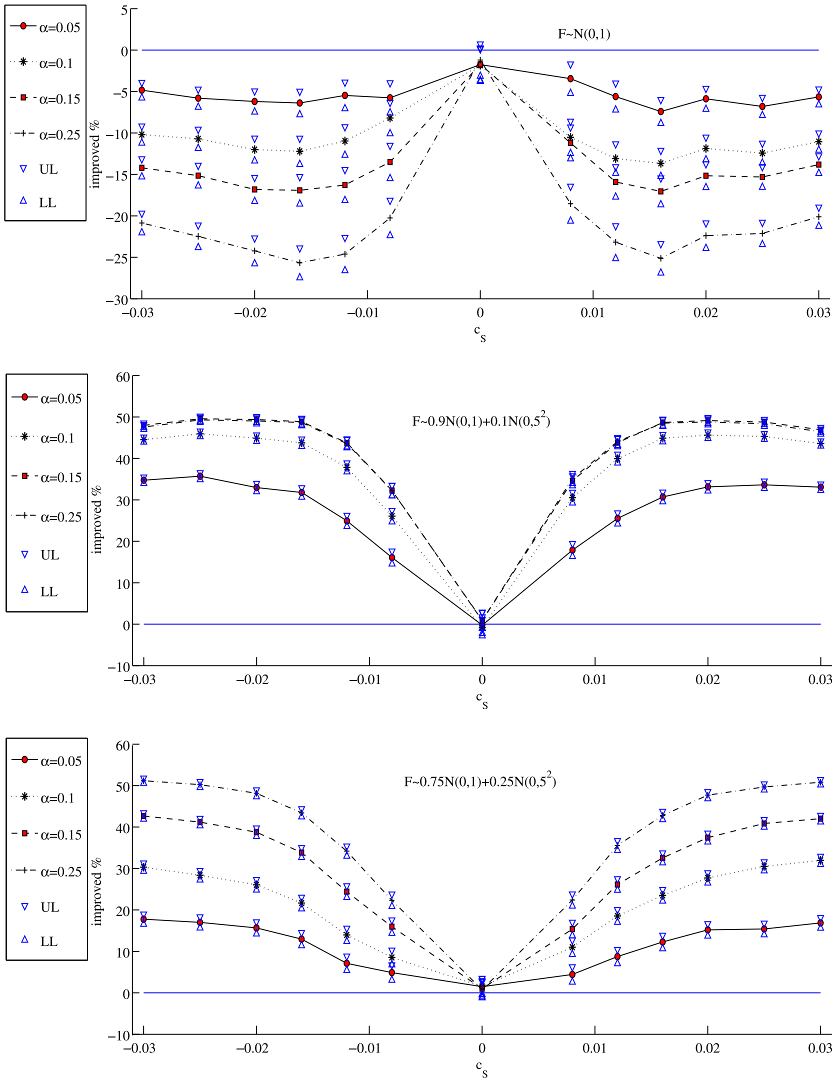

Figure 2. Improved percentages of the OC ARLs of the proposed charts for monitoring coefficient parameters when $\beta_1 \to \beta_1 + c_S$

standard deviation jointly, we substitute the term $Z_{PE,j}(\sigma)$ in (15) with $\alpha = 0$ for $Z_j(\sigma)$ in (9) in constructing the MEWMA chart of Zou *et al.*[9]because under the assumption that F has a contaminated normal distribution, the variance transformation (9) is obviously not appropriate and hence the original MEWMA chart is not feasible. Assume that when the process is in control, we have

$$y_{ij} = \beta_0 + \beta_1 x_i + \varepsilon_{ij}, i = 1, 2, \cdots, n, j = 1, 2, \cdots, \tag{19}$$

where $\beta_0 = 13, \beta_1 = 2$, and ε_{ij} has the distribution function F defined in (16). Here, we also assume that the sample size $n = 20$ and x_i, $i = 1, \ldots, 20$, are equally spaced values, -19, (2), 19. Note that except for larger sample size n, the underlying IC model is the same as that of Kang and Albin[1] with rescaling when $k = 0$. For monitoring the coefficient parameters only, Table III tabulates the upper control limits $H = L\lambda/(2-\lambda)$ and $H_{\boldsymbol{\beta}} = L_{\boldsymbol{\beta}}\lambda/(2-\lambda)$ of the MEWMA chart (without the $Z_j(\sigma)$ component) and the proposed chart, respectively, for IC ARL = 100, (k,b) = (0,1), (0.05, 3), (0.05, 5), (0.05, 10), (0.1, 5), (0.1, 10), (0.25, 5), (0.25, 10), α = 0.05, 0.1, 0.15, 0.25 and $\lambda = 0.02$ based on 50,000 simulations. Similarly, for monitoring both the coefficient parameters and standard deviation, Table IV displays the upper control limit $H = L\lambda/(2-\lambda)$ of the MEWMA chart and the upper control limits $H_{\boldsymbol{\beta}} = L_{\boldsymbol{\beta}}\lambda/(2-\lambda)$ and $H_\sigma = L_\sigma\lambda/(2-\lambda)$ of the proposed chart for IC ARL = 100, (k,b) = (0,1), (0.05, 3), (0.05, 5), (0.05, 10), (0.1, 5), (0.1, 10), (0.25, 5), (0.25, 10), α = 0.05, 0.1, 0.15, 0.25, and $\lambda = 0.02$ based on 50,000 simulations. For the proposed control chart, the individual IC ARL for the H_σ is about twice as large as that for the $H_{\boldsymbol{\beta}}$ such that the overall IC ARL = 100. It is also appropriate to set other different individual IC ARLs for the H_σ. It totally depends on how important that detecting a shift in σ is compared to that in a coefficient parameter. Note that we also simulated the upper control limits for several different parameter configurations from those in model (19) for the same IC ARL (not reported here). The results are quite similar to those tabulated in Tables III and IV. Hence, we conclude that the proposed control charts are parameter invariant approximately as long as the sample size n is not too small ($n \geq 20$). Figures 1 and 2 present the improved percentages of the out-of-control (OC) ARLs of the proposed charts with respect to those of the MEWMA charts for detecting shifts

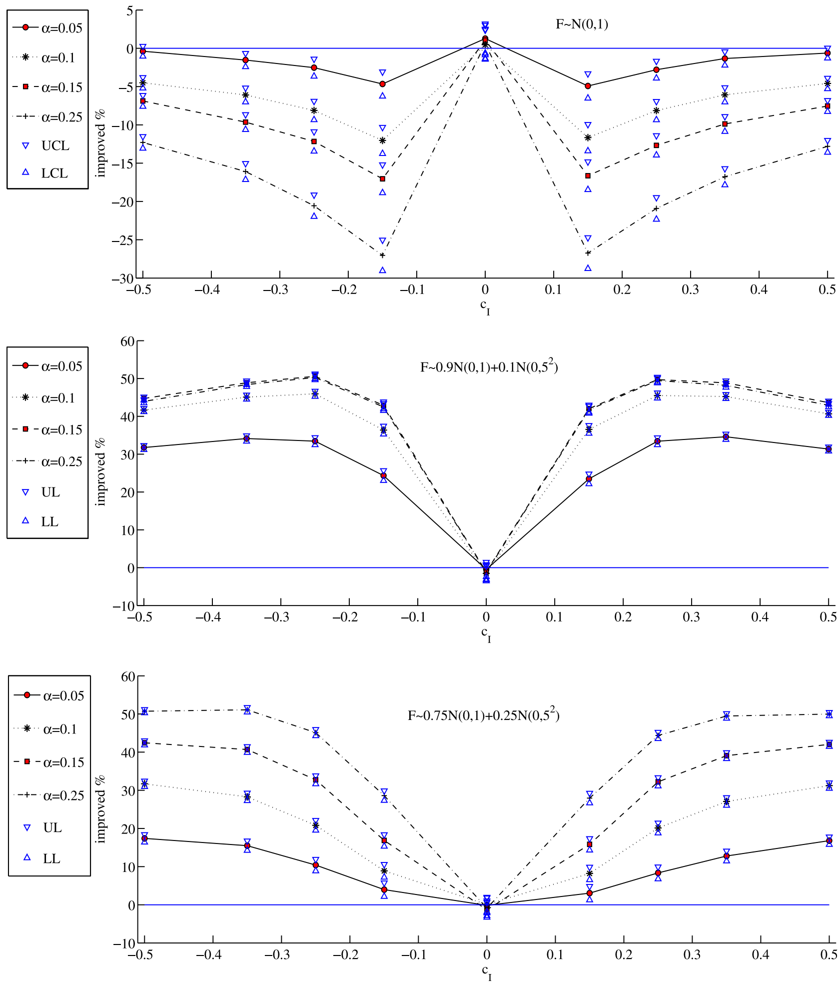

Figure 3. Improved percentages of the OC ARLs of the proposed charts for monitoring coefficient parameters and standard deviation simultaneously when $\beta_0 \rightarrow \beta_0 + c_l$

in β_0 and β_1, respectively. The 95% confidence intervals are also included (ULs and LLs in the figures). Precisely, the improved percentage is defined as the OC ARL of the MEWMA chart minus that of the proposed chart, and then divided by the OC ARL of the MEWMA chart. All the OC ARLs are computed based on 10,000 simulations. In this way, it is easy to judge how much improvement the proposed chart has attained. From the figures, we see that the proposed chart using the trimmed least squares estimator $\hat{\boldsymbol{\beta}}_{PE}(RQ(\alpha))$ outperforms the MEWMA chart when F has a contaminated normal distribution although it loses a little efficiency when F has a normal distribution. For example, when β_0 is changed to $\beta_0+0.15$, the OC ARL of the MEWMA chart equals 15.429 and that of the proposed chart equals 17.631 for $\alpha=0.1$ when $k=0$ (i.e. F has a standard normal distribution). On the other hand, the OC ARL of the MEWMA chart equals 34.119 (43.446, 58.984) and that of our proposed chart equals 21.101 (26.794, 49.410) for $\alpha=0.1$ when $(k, b)=(0.05,5)((0.1,5),(0.25,5))$ (i.e. F has a contaminated normal distribution).

For monitoring the coefficient parameters and the standard deviation simultaneously, Figures 3–5 present the improved percentages of the OC ARLs of the proposed charts with respect to those of the MEWMA charts for detecting shifts in β_0, β_1, and σ, respectively, based on 10,000 simulations. For detecting shifts in β_0 (β_1), Figure 3 (Figure 4) shows that the proposed chart performs uniformly better than the MEWMA chart when F has a contaminated normal distribution at the price that it gives slightly larger OC ARLs than the MEWMA chart when F has a normal distribution. As for monitoring σ, from the simulation results (not reported to save space), we see that the OC ARLs are not quite symmetric in detecting increase and decrease shifts for both the MEWMA and the proposed charts. In fact, both charts occasionally have biased results (OC ARL greater than IC ARL) in detecting decrease shifts in σ when F has a contaminated normal distribution although the proposed chart seems to be not as serious as the MEWMA chart. Note that in these cases, the advantage of the proposed chart over the MEWMA chart is significant in detecting decrease shifts but not in increase shifts. This results from the fact that the MEWMA charts is more biased than the proposed chart as it has a higher efficiency in detecting increase shifts than decrease shifts when F has a higher degree contaminated normal distribution.

In summary, when the distribution F of the random errors has a contaminated normal distribution, if $k \leq 0.05$ and $b \leq 5$, the proposed chart gives smaller OC ARLs with the trimmed proportion $\alpha=0.05$ or 0.1; if $k > 0.05$ or $b > 5$, the proposed chart performs much better with trimmed proportion $\alpha=0.15$ or 0.25 approximately. Practically, a better way to determine the value of the

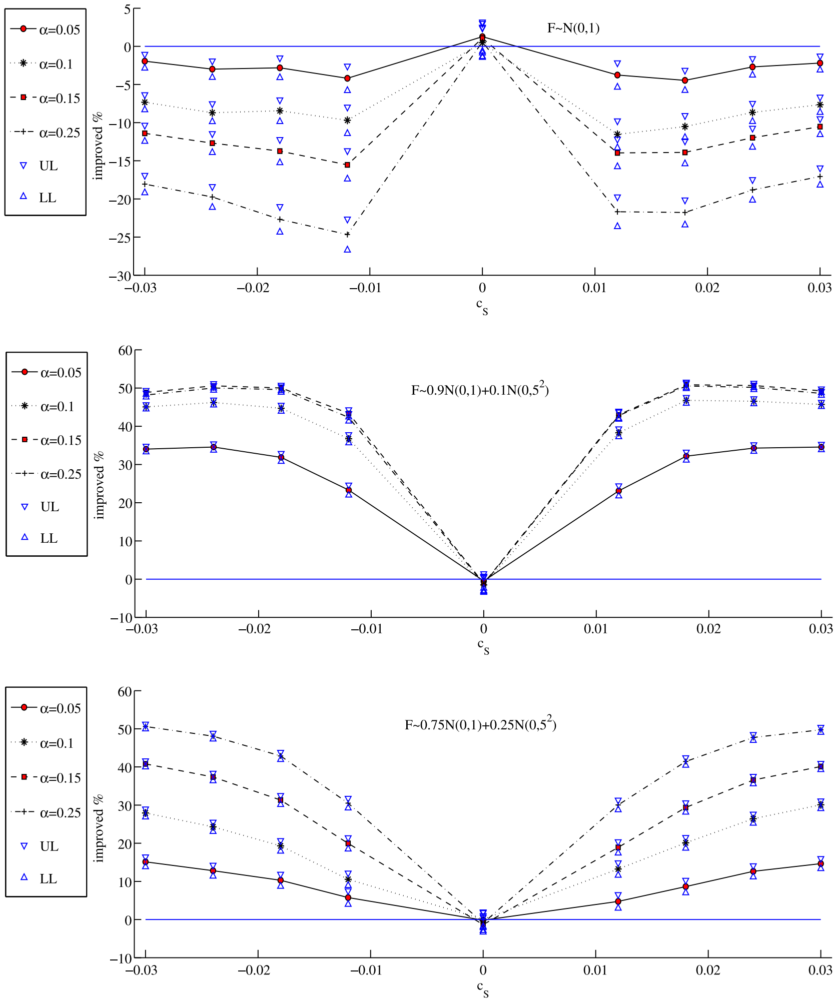

Figure 4. Improved percentages of the OC ARLs of the proposed charts for monitoring coefficient parameters and standard deviation simultaneously when $\beta_1 \rightarrow \beta_1 + c_S$

trimmed proportion α is to develop a data-driven methodology. However, this topic is beyond the scope of this research and is not pursued here.

We also simulated the performance of the proposed and MEWMA charts under the situation that $F \sim (1-k)N(\theta,\sigma^2) + kN(\varphi,\tau^2)$ where k is small, φ is quite different from θ, and τ is small (not reported here). The results are similar to above as long as $k \leq 0.2$ and the means θ and φ are, respectively, more than 3 standard deviations from the other normal distribution. Although in this situation, the distribution F generates outliers near the value φ and is not exactly symmetric, the proposed method still works satisfactory.

5. An illustrative example

In this section, we use a real dataset of general linear profiles where the random errors have contaminated normal distributions to illustrate how to implement the proposed charts in practice. This dataset was generated from a manufacturing process of aluminum electrolytic capacitors (AECs). It is concerned with the transformation of raw materials (anode aluminum oil, cathode aluminum foil, guiding pin, electrolyte sheet, plastic cover, aluminum shell, and plastic tube) into AECs which are suitable for use in low-leakage circuits and are well adapted to a large range environmental temperatures. The entire manufacturing process, which is also a multistage process, consists of a series of operations, such as clenching, rolling, soaking, assembly, cleaning, aging, and classifying (see Shi[39]). After each stage, the quality of capacitor elements, the unfinished AEC products, is examined by sampling according to its appearance and functional performance. Important characteristics of an AEC, for example, the dissipation factor and capacitance, are automatically calibrated via an electronic equipment at certain predetermined measuring voltage, frequency, and temperature. The general linear models (profiles) were commonly used in the literature to represent the relationship between the characteristics of the AEC from one stage to another stage (Shi[39]). Consequently, a remarkably change in the relationship may point out that the process is out of control. Note that Qiu *et al.*[28] and Zi *et al.*[29] also used different parts of this dataset to demonstrate profile monitoring although their methodologies emphasize on nonparametric approaches.

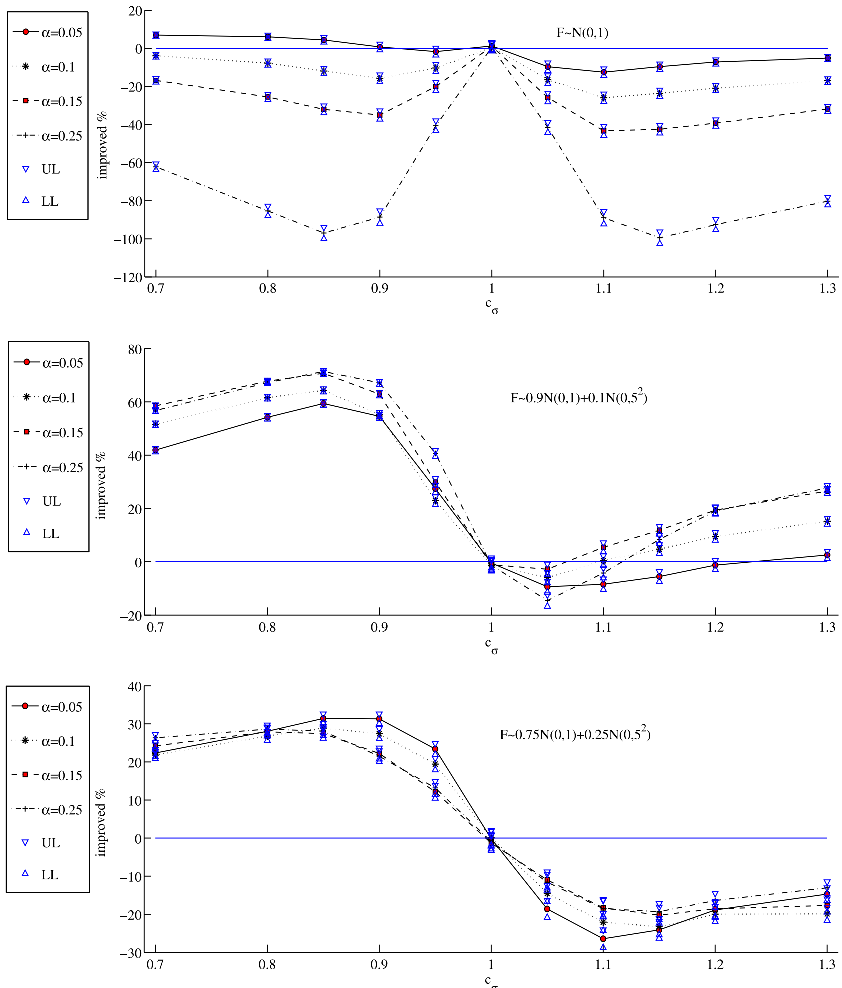

Figure 5. Improved percentages of the OC ARLs of the proposed charts for monitoring coefficient parameters and standard deviation simultaneously when $\sigma \rightarrow c_\sigma \sigma$

As illustrated by Zi *et al.*[29], the response variable y denotes the dissipation factor value in the aging stage and the independent variables x_1 and x_2 respectively represent the capacitance value and the dissipation factor observation from the soaking stage. There are totally 243 profiles of sample size 10. On the basis of physical knowledge and engineers' experiences, 227 out of 243 profiles are deemed as IC profiles and the other 16 profiles as OC (inferior) profiles. To simplify the data analysis, we only use 175 out of 227 profiles to demonstrate the proposed method in a realistic situation (the dataset is available on request). Since the independent variables $\mathbf{x}_i$ are not exactly the same for each of the 175 profiles, the 175 profiles are pooled together as a single sample. As a result, there are totally 1750 observations of y. Applying the ordinary least squares estimation to these data, we have the estimated IC profile

$$y_i = a + bx_{1i} + cx_{2i} + dx_{1i}^2 + \varepsilon_i, i = 1, \ldots, 10, \tag{20}$$

where $a = 26.210, b = 6.784, c = 3.848, d = 0.253$, and $\sigma_\varepsilon^2 = 0.341$. Note that although the above least squares estimates of the parameters are not most efficient, they are consistent estimates and based on such a large sample size, they should be very close

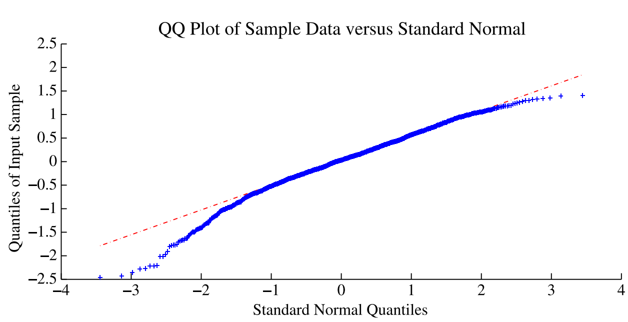

Figure 6. q – q plot for the residuals of the 175 in-control profiles

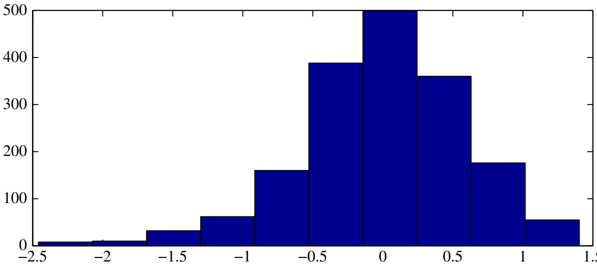

Figure 7. Histogram for the residuals of the 175 in-control profiles

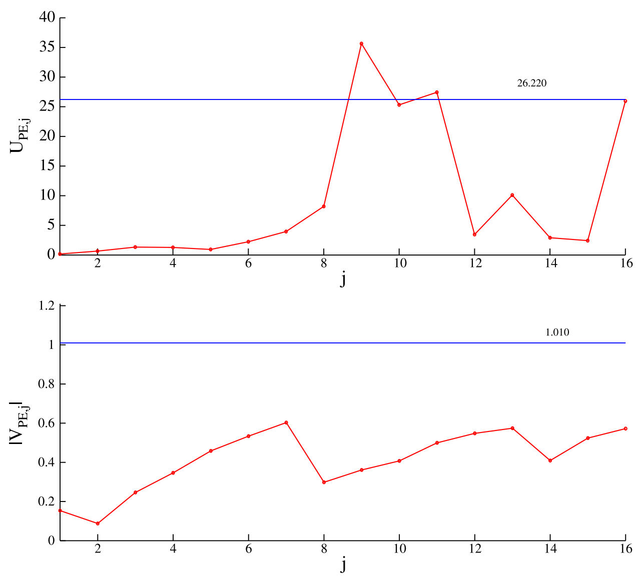

Figure 8. The proposed chart for monitoring the AEC profiles

to the unknown true parameters. As a result, we shall treat them as the true parameters of the IC process. To test the normality assumption on the error distribution, the chi-square statistic has p-value very close to 0. Consequently, the null hypothesis of normality on the error distribution is rejected. The $q-q$ plot and histogram of the residuals, presented in Figures 6 and 7, also confirm the result. Here, we use EM algorithm to classify the 1750 residuals into two groups. The means, variances, and proportions of the two groups are $\mu_1=0.064$ and $\mu_2=-1.540$, $\sigma_1^2=0.247$ and $\sigma_2^2=0.131$, and $1-k=0.96$ and $k=0.04$, respectively. The chi-square statistics for testing the normality assumption on these two groups have p-values 0.062 and 0.169, respectively (both do not reject the null hypothesis of being normal). The $q-q$ plot and histogram of the residuals also demonstrate the same results. This verifies that the random error has a contaminated normal distribution $F\sim 0.96N(0.064, 0.247)+0.04N(-1.540, 0.131)$. Note that the F may not be a fully ideal heavy-tailed distribution, it suffices to demonstrate the applicability of the proposed method because $k=0.04$ is small and the two group means, 0.064 and −1.540, are, respectively, more than 3 standard deviations from the other normal distribution. Furthermore, F has mean 0 and approximate symmetric distribution, and consequently, the trimmed least squares estimation which uses an effective preliminary estimator of the coefficient vector via the regression quantile introduced previously can be applied.

In this AEC process, the shift in regression coefficients may result in a different relationship between the dissipation factor values in the aging stage and the values of capacitance and dissipation factor observations in the soaking stage. On the other hand, an increase in standard deviation may indicate a rough profile or inaccuracies in the process and a decrease in standard deviation would illustrate an improvement in the process, as the regression coefficients do not shift. In the following, we shall use the proposed control charts to monitor the quadratic profile where the random error has a contaminated normal distribution to detect if there is any shift in the process parameters. Here, we will generate an OC scenario to demonstrate the applicability of the proposed and MEWMA charts.

First, we choose the IC ARL to be 100 and the smoothing constant $\lambda=0.2$. Subsequently, we obtain the upper control limits $H_{\boldsymbol{\beta}}=26.220$ and $H_\sigma=1.010$ for the proposed chart with trimming proportion $\alpha=0.1$ and the upper control limit $H=13.765$ for the MEWMA chart. Then, we construct the proposed and MEWMA charts for a Phase II monitoring. For the first four IC profiles, we generate profile data from model (20) with $\varepsilon_i\sim 0.96N(0.064, 0.247)+0.04N(-1.540, 0.131)$. Starting at the fifth profile, we add a shift of d on the IC model from 0.253 to 0.370 (about $0.2\sigma_\varepsilon$) and generate the OC profiles through Monte Carlo simulation. The simulated $y_{ij}, i=1,\ldots,10$ and $j=1,\ldots,16$ and the corresponding statistics $U_{PE,j}$ and $V_{PE,j}$ for the proposed chart and U_j for the MEWMA chart are presented in Table V.

Table V. IC and OC profiles and charting statistics for monitoring the AEC profiles

j						y_{ij}					U_j	$U_{PE,j}$	$\lvert V_{PE,j}\rvert$
1	10.85	13.50	15.94	18.81	23.83	25.65	30.04	36.22	42.21	47.05	0.17	0.18	0.15
2	10.13	12.33	16.64	18.59	24.24	26.08	29.80	35.29	43.01	48.01	0.79	0.66	0.09
3	10.95	13.80	16.47	19.44	23.12	25.99	30.81	35.83	40.24	47.47	1.87	1.34	0.25
4	11.06	12.39	17.15	19.91	23.60	25.64	29.79	36.69	40.57	47.31	1.75	1.28	0.35
5	9.71	12.00	17.03	18.63	24.33	24.98	32.16	36.06	42.25	46.95	1.57	0.93	0.46
6	11.26	12.19	16.33	19.33	22.71	25.55	31.16	36.13	42.16	47.27	1.63	2.24	0.53
7	9.93	12.71	15.88	18.90	23.40	26.23	30.24	37.51	42.43	46.88	2.29	3.96	0.60
8	8.91	13.16	16.45	18.64	23.51	24.98	29.65	37.70	42.58	48.51	3.09	8.20	0.30
9	9.88	12.93	15.48	17.40	23.71	25.69	29.88	37.46	43.27	48.41	12.94	35.64	0.36
10	10.50	13.00	14.80	18.02	23.07	26.27	30.78	37.77	42.24	47.64	10.58	25.32	0.41
11	9.61	11.30	15.91	18.53	23.63	26.01	31.24	36.97	42.48	48.43	13.65	27.43	0.50
12	10.14	12.32	15.79	19.08	23.13	25.31	30.94	36.56	43.25	47.60	3.37	3.46	0.55
13	10.42	11.45	14.67	19.21	24.73	25.07	30.22	35.85	43.66	48.81	8.91	10.11	0.57
14	9.82	12.98	15.03	19.34	25.01	25.84	30.96	35.75	41.88	47.50	2.95	2.92	0.41
15	10.30	13.61	16.09	18.90	23.43	25.52	31.17	36.15	41.41	47.52	2.48	2.43	0.52
16	10.11	12.93	15.37	18.45	23.74	25.62	30.30	36.75	42.91	47.91	22.31	25.97	0.57

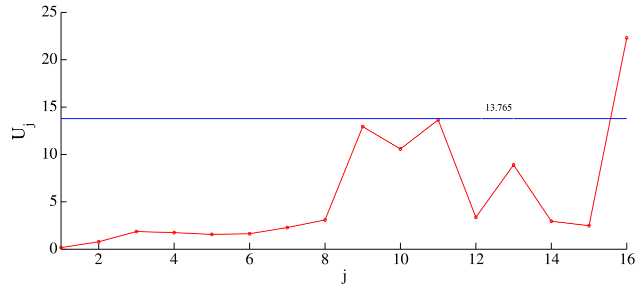

Figure 9. MEWMA chart for monitoring the AEC profiles

Figures 8, 9 give the proposed and MEWMA charts for monitoring these IC and OC sample profiles, where both control charts detect the changes in the coefficient parameters and standard deviation simultaneously. From the figures, we see that our proposed chart for monitoring the coefficient parameters detects an OC signal at profile 9 whereas the MEWMA chart triggers a signal at profile 16. For this artificial example, our proposed chart is more effective than the MEWMA chart by detecting the OC signal seven profiles earlier. It is worth noting that the magnitudes of shift in these profiles are usually small and difficult to identify by bare eyes. Therefore, we need an effective control chart to reveal small shifts in the profiles. After discovering the OC signal, users need to identify whether this is a true alarm or not. If yes, they may try to find the assignable causes and repair the process. The monitoring procedure for the AEC process can be restarted after the process has been adjusted back to normal conditions.

6. Conclusion

In this article, we have proposed a new control chart for monitoring the general linear profiles when the errors have contaminated normal distributions. The new control chart is based on the trimmed least squares estimation which makes use of an effective preliminary estimator of the vector of coefficient parameters through the regression quantile. On the basis of performance comparisons, the proposed chart outperforms the MEWMA chart when the errors have contaminated normal distributions at the price that it loses little efficiency when the errors have normal distributions. As illustrated by the AEC process, the proposed charting scheme can be practically applied in industry as the quality of a process can be described by a general linear profile with the error having a contaminated normal distribution. The future research which deserves further investigation is that how to estimate a changepoint in profile monitoring and identify the specific parameters in the profile that have changed when an OC signal is triggered by a control chart.

Acknowledgement

The authors would like to thank Professor Changliang Zou who kindly provided the dataset in the illustrative example and an anonymous referee for his many helpful comments that have resulted in significant improvements in the article. Huwang also acknowledges the support of NCTS of National Tsing Hua University in Taiwan.

References

1. Kang L, Albin SL. On-line monitoring when the process yields a linear profile. *Journal of Quality Technology* 2000; **32**:418–426.
2. Kim K, Mahmoud MA, Woodall WH. On the monitoring of linear profiles. *Journal of Quality Technology* 2003; **32**:317–328.
3. Gupta S, Montgomery DC, Woodall WH. Performance evaluation of two methods for online monitoring of linear calibration profiles. *International Journal of Production Research* 2006; **44**:1927–1942.
4. Croarkin C, Varner R. Measurement assurance for dimensional measurements on integrated-circuit photomasks. NBS Technical Note 1164, U. S. Department of Commerce.
5. Mahmoud MA, Woodall WH. Phase I monitoring of linear profiles with calibration application. *Technometrics* 2004; **46**:380–391.
6. Zou C, Zhang Y, Wang Z. Control chart based on change-point model for monitoring linear profiles. *IIE Transactions* 2006; **38**:1093–1103.
7. Mahmoud MA, Parker PA, Woodall WH, Hawkins DM. A change point method for linear profile data. *Quality and Reliability Engineering International* 2007; **23**:247–268.
8. Zou C, Zhou C, Wang X, Tsung F. A self-starting control chart for linear profiles. *Journal of Quality Technology* 2007; **39**:364–375.
9. Zou C, Tsung F, Wang Z. Monitoring general linear profiles using multivariate exponentially weighted moving average schemes. *Technometrics* 2007; **49**:395–408.
10. Jesen DR, Hui YV, Ghare PM. Monitoring an input–output model for production. I: The control charts. *Management Science* 1984; **30**:1197–1206.
11. Mestek O, Pavlik J, Suchanek M. Multivariate control charts: control charts for calibration curves. *Journal of Analytical Chemistry* 1994; **350**:344–351.
12. Stover FS, Brill RV. Statistical quality control applied to ionchromatography calibrations. *Journal of Chromatography. A* 1998; **804**:37–43.
13. Lawless JF, Mackay RJ, Robinson JA. Analysis of variation transmission in manufacturing process, Part I. *Journal of Quality Technology* 1999; **31**:131–142.
14. Wang YT, Huwang L. On the monitoring of simple linear Berkson profiles. *Quality and Reliability Engineering International* 2012; **28**:949–965.
15. Walker E, Wright S. Comparing curves using additive models. *Journal of Quality Technology* 2002; **34**:118–129.

16. Woodall WH, Spitzner DJ, Montgomery DC, Gupta S. Using control charts to monitor process and product quality profiles. *Journal of Quality Technology* 2004; **36**:309–320.
17. 17.Williams JD, Woodall WH, Birch JB. Statistical monitoring of nonlinear product and process quality profiles. *Quality and Reliability Engineering International* 2007; **23**:925–941.
18. Colosimo BM, Pacella M. On the use of principal component analysis to identify systematic patterns in roundness profiles. *Quality and Reliability Engineering International* 2007; **23**:707–725.
19. 19.Williams JD, Birch JB, Woodall WH, Ferry NM. Statistical monitoring of heteroscedastic dose–response profiles from high-throughput screening. *Journal of Agricultural, Biological, and Environmental Statistics* 2007; **12**:216–235.
20. Yeh AB, Huwang L, Li Y. Profile monitoring for a binary response. *IIE Transactions* 2009; **41**:931–941.
21. Shang Y, Tsung F, Zou C. Phase II profile monitoring with binary data and random predictors. *Journal of Quality Technology* 2011; **43**:196–208.
22. Jin J, Shi J. Feature-preserving data compression of stamping tonnage information using wavelet. *Technometrics* 1999; **41**:327–339.
23. Lada EK, Lu JC, Wilson JR. A wavelet-based procedure for process fault detection. *IEEE Transactions on Semiconductor Manufacturing* 2002; **15**:79–90.
24. Ding Y, Zeng L, Zhou S. (2006) Phase I analysis for monitoring nonlinear profiles in manufacturing processes. *Journal of Quality Technology* 2006; **38**:199–216.
25. Zou C, Tsung F, Wang Z. Monitoring profiles based on nonparametric regression methods. *Technometrics* 2008; **50**:512–526.
26. Fan J, Zhang C, Zhang J. Generalized likelihood ratio statistics and Wilks phenomenon. *The Annals of Statistics* 2001; **29**:153–193.
27. Fan J, Gijbels I. Local Polynomial Modeling and Its Applications. Chapman & Hall: London, 1996.
28. Qiu P, Zou C, Wang Z. Nonparametric profile monitoring by mixed effects modeling. *Technometrics* 2010; **52**:265–293.
29. Zi X, Zou C, Tsung F. A distribution-free, robust method for monitoring linear profiles using rank-based regression. *IIE Transactions* 2012; in press.
30. Lehmann EL. Theory of Point Estimation. Wiley: New York, 1983.
31. Stigler SM. Do robust estimators work with real data? *The Annals of Statistics* 1977; **5**:1055–1098.
32. Koenker R, Bassett GJ. Regression quantiles. *Econometrica* 1978; **46**:33–50.
33. Koenker R. Galton, Edgeworth, Frisch, and Prospects for quantile regression in Econometrics. *Journal of Econometrics* 2000; **95**:347–374.
34. Koenker R, Hallock K. Quantile regression. *Journal of Economic Perspectives* 2001; **15**:143–156.
35. Meketon M. Least absolute value regression. AT & T Bell Laboratories, Holmdel, NJ, 1986.
36. Rupport D, Carroll R. Trimmed least squares estimation in the linear model. *Journal of the American Statistical Association* 1980; **75**:828–838.
37. Lowry CA, Woodall WH, Champ CW, Rigdon SE. A multivariate exponentially weighted moving average control chart. *Technometrics* 1992; **34**:46–53.
38. Prabhu SS, Runger GC. Designing a multivariate EWMA control chart. *Journal of Quality Technology* 1997; **29**:8–15.
39. Shi J. Stream of Variation Modeling and Analysis for Multistage Manufacturing Processes. CRC Press: Florida, 2007.

Authors' biographies

Longcheen Huwang received his PhD in Statistics from Cornell University in 1991. He is currently a Full Professor at the Institute of Statistics, National Tsing Hua University, Hsinchu, Taiwan. He is an elected member of International Statistical Institute. His research includes quality management and statistical inference.

Yi-Hua Tina Wang received her PhD in Statistics from the Institute of Statistics, National Tsing Hua University, Hsinchu, Taiwan in 2010. She is currently an assistant professor in the Department of Statistics of Tamkang University, Taiwan. Her research interest includes data mining and industrial statistics. Her email address is 141110@mail.tku.edu.tw.

Cheng-Che Shen received his Master degree in Statistics from the Institute of Statistics, National Tsing Hua University, Hsinchu, Taiwan.He is currently an engineer at a private industrial company in Hsinchu, Taiwan.